Development of High-Speed and High-Voltage Pulse Generator for NO_x Decomposition Plasma Reactor

Toshihiko Noguchi, Hafidz Elmana, Ryota Kitamoto and Kazuki Shimizu
Shizuoka University
noguchi.toshihiko@shizuoka.ac.jp, hafidz.elmana.16@shizuoka.ac.jp

***Abstract*-This paper proposes a novel high-speed and high-voltage pulse generator for a NO_x decomposition plasma reactor for automotive application, which is composed of a DC/DC step-up converter and a multiple-toroidal-core technique. The DC/DC converter steps up 12-V battery voltage to 420 V with an isolated high-frequency transformer. 12 ferrite toroidal cores are connected to the output of the DC/DC converter, and they are simultaneously excited by turning on 12 MOSFETs. The synchronous switching is achieved within only ±2-ns time deviation. The secondary high-voltage winding is placed through the 12 toroidal cores, and generates 10,000 V across the terminals in 50 ns. In order to make this high-speed and high-voltage pulse generation possible, the system has unique configuration and special appearance. In the paper, an experimental prototype and test results are demonstrated to show the performance of the proposed system.**

I. INTRODUCTION

In recent years, various regulations for environmental conservation are imposed as environmental pollution is getting a serious matter. Many sorts of research and development activities are promoted to satisfy the requirements of the regulations. In some part of the metropolitan areas in some developed countries, it is mandatory to mount an exhaust depurator on a vehicle to decompose nitrogen oxide (NO_x) contained in the exhaust gas from a diesel engine. NO_x is an air pollution material that causes photochemical smog and acid rain not only in urban areas but also in rural areas. Particularly, high-density nitrogen dioxide (NO_2) is strictly restricted by the environmental standard because it affects detrimentally respiratory organs of human being [1].

Market of diesel engine based vehicles is growing in the developed countries such as Japan and Western European countries, where the brand-new vehicles are sold with so-called clean diesels. In general, diesel engine vehicles can deliver higher torque and reduce the carbon dioxide (CO_2) emission, resulting in higher combustion efficiency with lower fuel consumption, compared with gasoline based vehicles. However, it is still demanded to improve the diesel engine performance, especially quality of exhaust gas that contains NO_x and particulate matters, acoustic noise, mechanical vibration and so forth. There have been many methods reported to decompose NO_x and its relevant materials as follows: 1) a selective catalytic reduction (SCR) method which employs carbon hydride as catalyst; 2) decomposition method of nitrous oxide (N_2O) which is a by-product of SCR process; and 3) a low-temperature plasma decomposition method using corona discharge [2] [3].

This paper focuses on the low-temperature plasma decomposition method, and an application of power electronics is attempted to generate ultra-high-speed high-voltage pulse for the plasma reactor. It is already known that the low-temperature plasma decomposition method requires high-voltage pulse generator, of which rise time of the voltage pulse is a key factor for efficient decomposition quantity of NO_x. It is reported that decomposition rate of NOx can be over 95 % by achieving high-rise-time within 100 ns, high-peak-voltage over 10 kV, and repetitive period of 1 kHz, for example. In addition, other most important points are physical dimensions of the equipment and the power source voltage because both of them are severely restricted to implement on the actual vehicle. The transformer in the newly developed high-speed and high-voltage pulse generator employs a toroidal multi-core approach to optimize placement of the transformer cores and to reduce the line inductance to obtain less than 100-ns rise time and higher than 10-kV peak voltage [4]-[7]. The paper discusses practical implementation techniques to reduce the line inductance, to achieve simultaneous high-speed switching of multiple parallel-connected MOSFETs, and to make the compact mechanical configuration possible. Feasibility of the developed system has been confirmed through experimental tests using a prototype, which proves usefulness of the proposed approach [8].

II. DESIGN OF HIGH-SPEED AND HIGH-VOLTAGE PULSE GENERATOR USING TOROIDAL MULTI-CORE TRANSFORMER

Fig. 1 and TABLE I show a main circuit schematic diagram and its components of the high-speed and high-voltage pulse generator. As can be seen in the figure, the voltage boost is achieved by using a two-stage configuration. The first stage employs a combination of a push-pull DC/DC converter and a high-frequency step-up transformer, and the second stage uses a toroidal multi-core transformer with connecting its primary side in parallel and its secondary side

978-1-5090-2364-6/17/$31.00 ©2017 IEEE

like in series. The primary sides of the toroidal multi-core transformer have the high-speed switching devices to magnetize the multiple cores simultaneously.

The voltage is stepped up through the first stage from 12 VDC to 420 VDC. The push-pull inverter has a 12-V automotive battery as a power supply, and operates at the frequency of 50 kHz to step up the voltage. The inverter output is connected to the ferrite core step-up transformer, whose turn ratio is 35. A simple full-bridge diode rectifier is used to obtain the DC bus voltage V_1 followed by a LC filter. On the second stage, MOSFETs Q_1-Q_{12} are employed to achieve simultaneous switching, and are connected to the primary windings of the toroidal multi-core transformer. There are twelve ferrite toroidal cores used as a transformer. Their primary windings are connected to the MOSFETs one by one. On the other hand, a single secondary winding is wound around through the twelve ferrite toroidal cores in a torus shape. The total voltage step-up ratio of the second stage is 24 times. All of the twelve MOSFETs Q_1-Q_{12} are turned on for 500 ns every 1 ms, and generate high-speed and high-voltage pulse across the secondary winding terminals. The following equations are used for the design of the toroidal multi-core transformer:

$$V_1 = \frac{2}{D} B_m S N_1 f \text{ , and} \tag{1}$$

$$V_2 = n\frac{2}{D} B_m S N_2 f \text{ ,} \tag{2}$$

where V_1 is a primary voltage, V_2 is a secondary voltage, N_1 is a primary number of turns, N_2 is a secondary number of turns, B_m is magnetic flux density, S is a section area of the transformer, f is an operating frequency, n is a toroidal core count. As indicated in (2), n-times high-voltage can be obtained on the secondary winding because the secondary side of each toroidal core can be regarded to be equivalent to the series connection. Major design parameters of the prototype are listed in TABLE II.

The peak voltage of the output pulse can be determined by the turn ratio of the transformer and the number of the toroidal cores. Assuming that the transformer is ideal, the relationship between the primary and the secondary voltages are simply expressed as

$$V_2 = n\frac{N_2}{N_1} V_1 . \tag{3}$$

The transformer employs the ferrite toroidal cores in order to improve the frequency characteristics and to reduce the leakage inductance at the same time.

III. Implementation of Prototype with Low Inductance for High-Speed Switching

A. Required Specifications and Reduction of Inductance

It is required for the prototype to satisfy the voltage rise time less than 100 ns to the peak over 10 kV because the higher the rise time is, the more the NO_x can be decomposed.

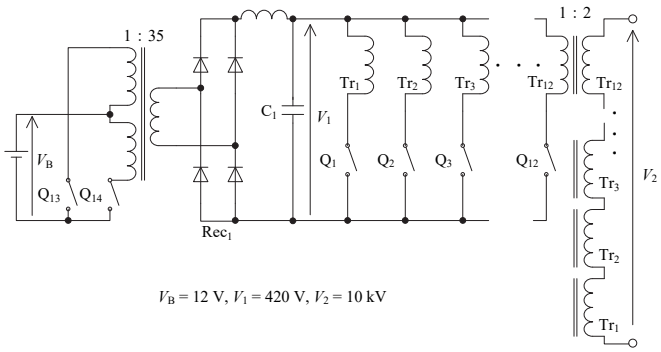

Fig. 1. Configuration of main circuit.

TABLE I Components in Main Circuit.

Symbols	Components	Specifications	Quantities
Q_1-Q_{12}	DE375-102N12A	1000 V, 12 A t_{on}: 3 ns	12
Q_{13} and Q_{14}	IRFB61N15D	150 V, 60 A	2
Rec_1	FMG-G2CS	1000 V, 30 A	4
C_1	EMC	600 V, 100 μF	2
Tr_1-Tr_{12}	PC95	T38×14×22	12

TABLE II Design Parameters of Toroidal Multi-Core Transformer.

Parameters	Symbols	Values
Primary voltage	V_1	420 V
Secondary voltage	V_2	10×10^3 V
Primary number of turns	N_1	4
Secondary number of turns	N_2	8
Number of multiple cores	n	12
Duty cycle	D	0.005
Magnetic flux density	B_m	0.5 T
Section area	S	112×10^{-6} m^2
Operation frequency	f	1×10^3 Hz

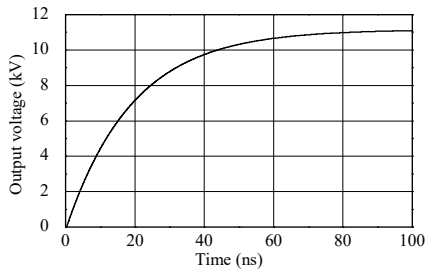

Fig. 2. Simulation result of output pulse transient behavior.

Therefore, it is indispensable to reduce the line inductance disturbing the high-speed switching. Fig. 2 shows a computer simulation result to check the influence of the line inductance to the voltage rise time. The simulation was conducted with an ideal transformer with the primary windings connected in parallel and the secondary windings connected in series to generate over 10 kV pulse. By intentionally inserting the line inductance to the ideal transformer, the maximum value of the line inductance was found to satisfy the required specifications. As can be found in Fig. 2, 10-kV output within 50 ns is possible by limiting the line inductance less than 100 nH.

B. Reduction of Inductance by Means of Optimized Implementation of Components

As Fig. 1 shows, each of twelve toroidal cores Tr_1-Tr_{12} is connected to and is switched over by one of the twelve MOSFETs Q_1-Q_{12}. The line inductance can be reduced by placing the toroidal core close to the switching device. The twelve MOSFETs must be turned on at the almost same time, so the MOSFETs and their drive circuits are placed in a ring shape to make the current path perfectly symmetrical. In addition to that, the front and the rear sides of the printed wire board (PWB) are used for the current path, and the line inductance is effectively reduced by making the current flow in opposite directions on the both sides. Furthermore, the main current root is separated from the gate drive circuit to prevent the conduction noise caused by the MOSFETs to the gate drive ICs. Fig. 3 shows turn-on waveforms of the MOSFETs, where the twelve waveforms are synchronously measured and are superimposed in the figure. It is confirmed from the figure that all of the waveforms turn on within the 1-ns time deviation.

C. Reduction of Inductance with Multi-Core Transformer

Fig. 4 illustrates a CAD model that has a winding configuration employed in the prototype. In the second stage step-up transformer, each primary winding is wound around a toroidal core, respectively, and the secondary winding is wound through all the twelve toroidal cores in a torus shape. It is impossible to draw the electric circuit diagram of the secondary winding connection of the multi-core transformer; hence, Fig. 1 does not reflect the actual winding configuration. Taking this configuration contributes to enhance the magnetic coupling, which leads to efficient reduction of the leakage inductance. TABLE III shows specifications of the windings. Because a high-withstanding voltage is required on the secondary winding, a 30-kV electric wire with silicon insulator is employed. The silicon sheath is mechanically flexible enough to wind around the wire through the multiple toroidal cores with a high-space factor, which also effective to increase the magnetic coupling coefficient.

D. Compact Design with 3D CAD

Fig. 5 illustrates a CAD model of the prototype, which has been designed to make the total volume minimum, assuming an actual application to the automotives. In order to make every wiring as short as possible, the first and the second stages are stacked up in the vertical way. The push-pull DC/DC converter and the LC filter across the DC bus are placed under the PWB, while the toroidal multi-cores are placed on the PWB. As described previously, the wire length between the MOSFETs and the toroidal core is as short as 10 mm. The dimensions of the whole system are 200 mm in diameter and 135 mm in height, and the weight is approximately 2 kg, which allows mounting this system close to the actual automotive exhaust system. Since the wire length at every part is designed as short as possible owing to the optimized configuration described above, the turn-off serge voltage across the DC bus due to the line inductance can be reduced down to 5 % of the DC bus voltage.

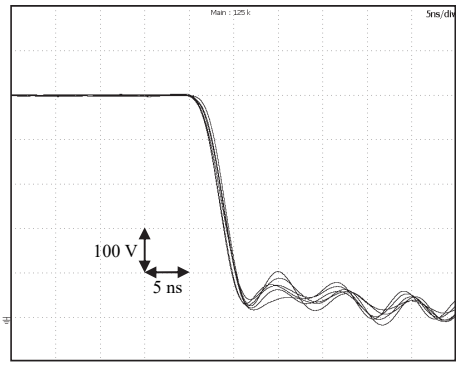

Fig. 3. Turn-on waveforms of MOSFETs.

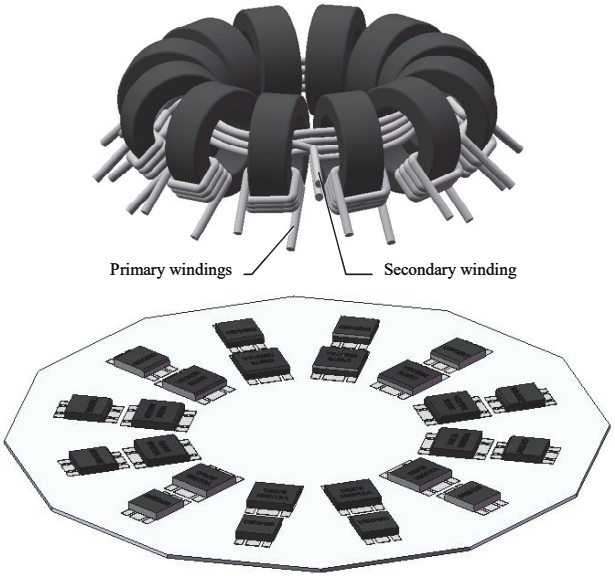

Fig. 4. Winding configuration of toroidal multi-core transformer.

TABLE III SPECIFICATIONS OF WINDING.

Windings	Components	Voltage ratings	Outer diameter of conductors
Primary winding	C3/RV-90 LF	2000 V	1.3 mm
Secondary winding	UL3239	30 kV	2.0 mm

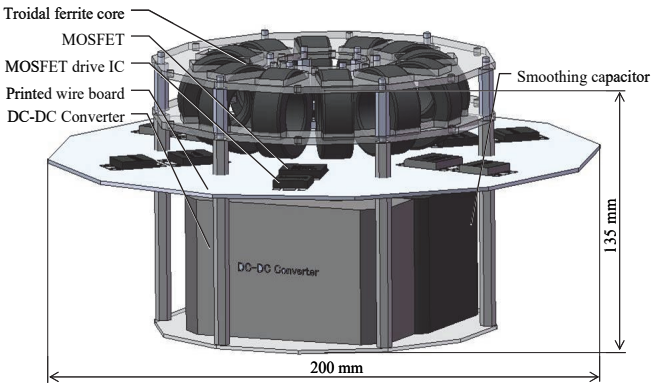

Fig. 5. Overview of high-speed and high-voltage pulse generator prototype.

IV. PROTOTYPE AND EXPERIMENTAL TEST RESULTS

A. Prototype

Fig. 6 shows photographs of the high-speed and high-voltage pulse generator prototype. TDK PC95 T38x14x22 ferrite toroidal cores are selected on the basis of the design parameters calculated by (1)-(3), and are employed in the prototype. The turn ratio of the second stage multi-core transformer is 4:8. Since the number of toroidal cores is twelve, the voltage step-up rate of the second stage is 12*8/2 = 24 times.

Several experimental tests have been conducted to examine the operation characteristics, using the prototype. In the following sections, feasibility of the design is verified through the test results.

B. Output Voltage Characteristic with Respect to Toroidal Core Counts of Multi-Core Transformer

Experimental tests have been conducted with changing the toroidal core counts of the multi-core transformer to 4, 6, 8, and 12 under a condition of a 420-VDC constant DC bus voltage and a 4:8 constant turn ratio. The peak value and the rise time of the output voltage are shown in Figs. 7 and 8, respectively. As described in the previous sections, the output voltage can be adjusted not only by changing the turn ratio but also by changing the number of the toroidal cores used. It is found that the output voltage is proportional to the toroidal core counts from (2) and (3), but the rise time of the voltage pulse is supposed to be longer as the number of the toroidal cores increases because of more leakage magnetic flux or more leakage inductance. Increasing the number of turns can detrimentally affect the leakage inductance, resulting in the slow voltage rise due to the longer time constant determined by the leakage inductance.

It can be found from Fig. 7 that 4.5-kV is available across the output terminals even though the toroidal core counts are four. The theoretical value of the output peak voltage is 3.4 kV, and the actual value is higher than the theoretical one because of the serge voltage imposed on the output. As the number of the toroidal cores is increased, however, the output voltage is also proportionally increased as the theoretical expressions suggest. Fig. 8 represents that the rise time of the output voltage is also almost proportional to the toroidal core counts. This is because of the larger leakage inductance depending on the secondary wire length that is proportional to the number of toroidal cores. As Fig. 8 demonstrates, the rise time is only 50 ns even when the toroidal core counts are twelve to generate over 10-kV peak output voltage.

C. Output Voltage Characteristic with Respect to Primary DC Bus Voltage

Other experimental tests have been conducted with changing the primary DC bus voltage to 100 V, 200 V, 300 V, and 420 V under a condition of the twelve toroidal cores used in the multi-core transformer and their 4:8 constant turn ratio. Figs. 9 and 10 show the characteristics of the output peak voltage and the rise time, respectively. As (3) indicates, the output voltage increases as the primary voltage increases if the turn ratio and the toroidal core counts are fixed at constant values. It is confirmed in Fig. 9 that the output peak voltage is proportionally increases as the primary DC bus voltage is increased. However, every output peak voltage value is slightly higher than the theoretical value because the serge

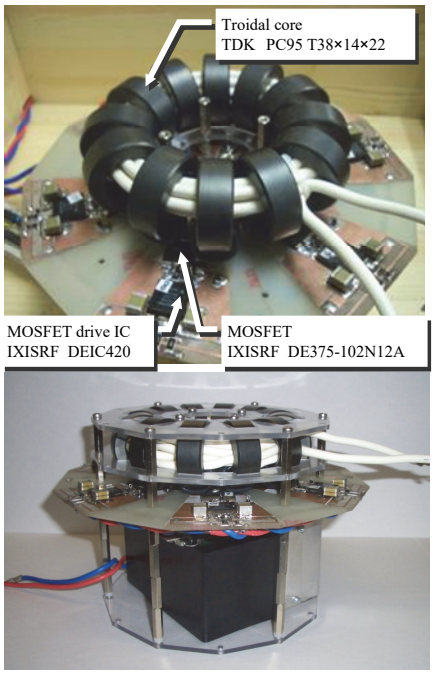

Fig. 6. Photographs of prototype.

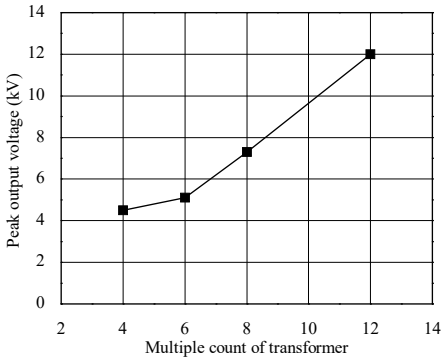

Fig. 7. Characteristic of output peak voltage with respect to toroidal core counts of multi-core transformer.

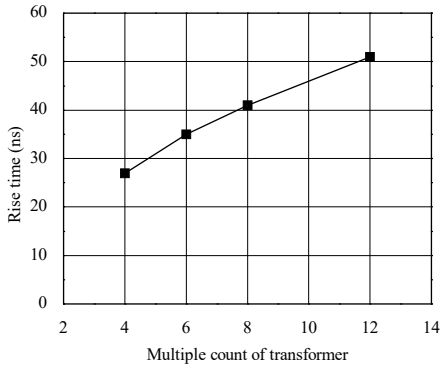

Fig. 8. Characteristic of output voltage rise time with respect to toroidal core counts of multi-core transformer.

voltage pushes up the voltage level as explained previously. As for the rise time of the output voltage pulse, it is known that the rise time is slightly affected by the primary DC bus voltage. This rise time variation seems to be caused by the constant load resistance. In other words, increased load current caused by the increased primary DC bus voltage and the constant load resistance makes the rise time slightly longer. However, the difference of the rise time between 100-V and 400-V DC bus voltages is only 6 ns; hence it can be confirmed that the load current value hardly affects the rise time.

D. Output Voltage Characteristic with Respect to Load Resistance

Other experimental tests have been conducted with changing the load resistance to 2.8 kΩ, 5.6 kΩ, 8.4 kΩ, and 11.2 kΩ under the condition of the twelve toroidal cores used in the multi-core transformer, their 4:8 constant turn ratio, and 420-V constant primary DC bus voltage. The peak value and the rise time of the output voltage are shown in Figs. 11 and 12, respectively. Fig. 11 shows the output peak voltage is kept almost constant over 10 kV regardless of the load resistance. The rise time of the output voltage pulse can also be found to be almost constant around 50 ns despite the load resistance variation. From these characteristics, it is confirmed that the output voltage characteristics are hardly affected by the load current, which implies that the internal impedance of the designed prototype is quite low. The MOSFETs used in the experimental tests have the drain current rating of 12 A because the 3-kΩ load resistance is assumed for an actual plasma reactor application. If the MOSFETs have the higher current rating, more instantaneous power can be obtained by reducing the load resistance value as long as the MOSFETs have similar switching speed as those used in the prototype.

An output voltage pulse train waveform is shown in Fig. 13, and its expanded waveform is shown in Fig. 14, which has been measured in the experimental tests under the condition of the twelve toroidal cores used in the multi-core transformer, their 4:8 constant turn ratio, 420-V constant primary DC bus voltage, and 5.6 kΩ load resistance. It is confirmed from these results that the 1-ms cyclic voltage pulse with as fast rise time as 50 ns and as high voltage as 10 kV is obtained with the prototype.

E. Energy Conversion Efficiency and Power Consumption

Fig. 15 shows efficiency characteristic with respect to the load power. Efficiency of the DC/DC converter in the first voltage step-up stage reaches 80 % when the load is relatively heavy, while the efficiency of the second voltage step-up stage is around 57 % at the same load. Therefore, the total efficiency is 47 % at most. The reason why the second stage has such low efficiency is as follows:

1) switching loss of the MOSFETs;
2) conduction loss caused by on-voltage of the MOSFETs;

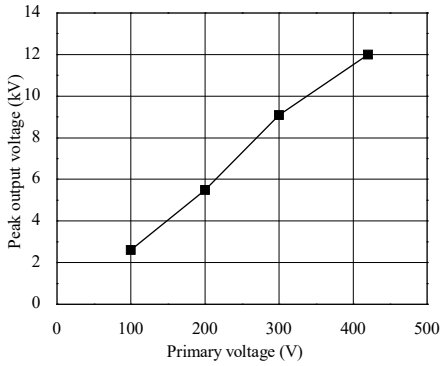

Fig. 9. Characteristic of output peak voltage with respect to primary DC bus voltage.

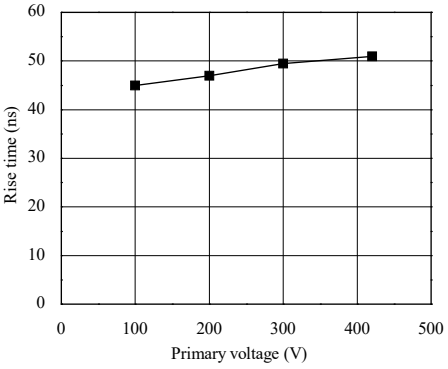

Fig. 10. Characteristic of output voltage rise time with respect to primary DC bus voltage.

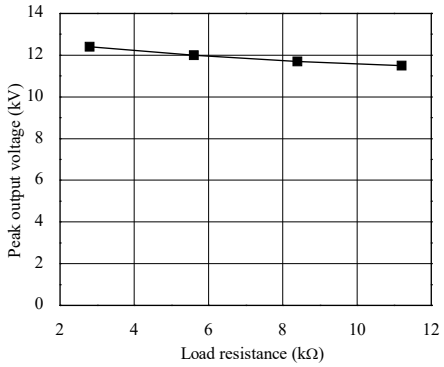

Fig. 11. Characteristic of output peak voltage with respect to load resistance.

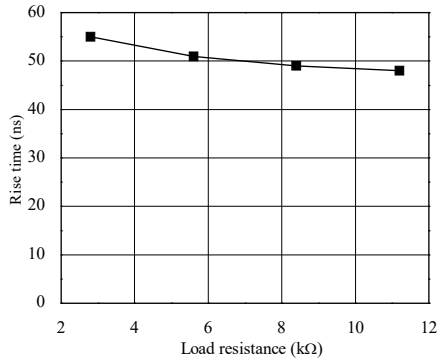

Fig. 12. Characteristic of output voltage rise time with respect to load resistance.

3) power loss in the snubber circuits; and
4) iron loss in the toroidal multi-cores.

The major part of the total power loss is occupied by the snubber loss and the conduction loss of the MOSFETs. It is necessary to investigate the power loss further and to improve the total efficiency in the future work.

F. Discussion on Output Voltage Characteristics

The experimental test results demonstrated output voltage characteristics with the rise time less than 100 ns to reach 10 kV, which proves feasibility of the design approach. However, it has been confirmed through the tests that the rise time becomes longer as the number of the toroidal multi-cores increases, which has an opposite trend, compared with the experimental results confirmed in the past study of the authors' [4]. The difference between the current prototype and the past model is the number of turns on the secondary side in the toroidal multi-core transformer. In the experimental tests described in this paper, the number of turns is fixed at eight regardless of the toroidal core counts. In the past tests, however, as the toroidal core counts increase, the secondary number of turns is reduced to keep the magnetic flux density in each toroidal core constant. In other words, as more toroidal cores are used, the length of the secondary wire becomes longer in this paper, but becomes shorter in the past test results. Therefore, the length of the secondary winding in the toroidal multi-core transformer is a dominant factor to influence the rise time of the output voltage pulse. It is important to take balance between the secondary number of turns and the number of the toroidal cores for boosting up the voltage and to reduce the secondary number of turns as low as possible to speed up the voltage rise. In addition to that, a voltage oscillation of 4 MHz is observed in Fig. 14 when the toroidal core counts are increased to twelve. This oscillation is supposed to be generated by the resonance between the line inductance and the stray capacitance. The more the toroidal cores are connected, the more the stray capacitance comes into prominence.

V. CONCLUSION

This paper discussed a compact high-speed and high-voltage pulse generator for a NO_x decomposition plasma reactor. The target application of the pulse generator is an exhaust depurator for automotives. The pulse generator takes advantage of the two-stage voltage step-up configuration and the toroidal multi-core transformer in the second stage to achieve ultra fast rise time less than 100 ns to reach over 10-kV output voltage. It has been confirmed through several experimental tests that the pulse generator prototype achieved as fast-rise-time as 50 ns and as high-voltage as 12 kV almost regardless of the load current.

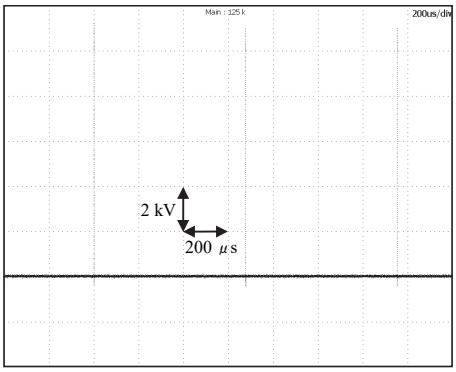

Fig. 13. Output voltage pulse train waveform.

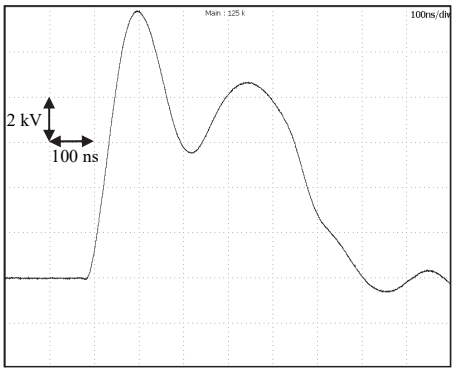

Fig. 14. Expanded waveform of output voltage.

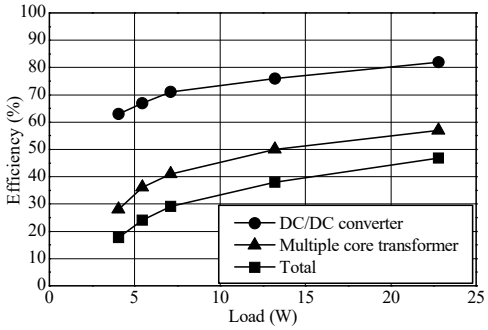

Fig. 15. Efficiency characteristic with respect to load power.

REFERENCES

[1] White Paper and Annual Report on the Environment and Sound Material Cycle Society in Japan, Ministry of the Environment.

[2] Search Zn, Al, Rh-Mixed Oxides Derived from Hydrotalcite-Kike Compound and Their Catalytic Properties for N_2O Decomposition, *Applied Catalysis B: Environmental*, vol.13, 1997, pp. 197-203.

[3] Formation of Nitroethylene during Selective Catalytic Reduction of NO_2 by C_2H_4 over H-Ferrierite, *Chemical Communications*, 2000, pp. 173-174.

[4] H. Maeoka and T. Noguchi, "High-Voltage Pulse Power Supply Using Multiple Transformers with Novel Winding Structure," *IEEJ Vehicle Technology Technical Meeting*, VT-05-7, 2004, pp. 37-42.

[5] N. Tsuji and S. Kondo, "Development of High Efficiency Low-Voltage / High-Current DC Power Supply," *IEEJ Semiconductor Power Conversion Technical Meeting,* SPC-03-141, 2003, pp. 45-50.

[6] I. Takahashi, "Project of Next^2 Generation D-D Converters: Proposal of a Switching Power Supply of Next^2 Generation," *IEEJ National Convention Record*, 4-030, 2003, pp. 36.

[7] H. Maeoka and T. Noguchi, "Study on Windings Structure and Output Characteristics of Multiple Transformers in High-Voltage Pulse Power Supply," *IEEJ Transactions on Industry Applications*, vol. 1, 2004, pp. 487-488.

[8] R. Kitamoto and T. Noguchi, "10 kV-50 ns Pulse Power Supply Using Ultra High-Speed Switching Devices and Toroidal Multiple Cores," *IEEJ Semiconductor Power Conversion Technical Meeting*, SPC-09-87, 2009, pp. 45-50.